AIP | The Journal of Chemical Physics

The contribution of the delayed ionization in strong-field nonsequential double ionization

Yinbo Chen, Yueming Zhou, Yang Li, Min Li, Pengfei Lan, and Peixiang Lu

Citation: The Journal of Chemical Physics **144**, 024304 (2016); doi: 10.1063/1.4939642
View online: http://dx.doi.org/10.1063/1.4939642
View Table of Contents: http://scitation.aip.org/content/aip/journal/jcp/144/2?ver=pdfcov
Published by the AIP Publishing

Articles you may be interested in

Strong-field ionization rates of linear polyenes simulated with time-dependent configuration interaction with an absorbing potential
J. Chem. Phys. **141**, 174104 (2014); 10.1063/1.4900576

Strong-field induced XUV transmission and multiplet splitting in 4d −16p core-excited Xe studied by femtosecond XUV transient absorption spectroscopy
J. Chem. Phys. **137**, 244305 (2012); 10.1063/1.4772199

Nonadiabatic theory of strong-field atomic effects under elliptical polarization
J. Chem. Phys. **137**, 22A542 (2012); 10.1063/1.4752079

Strong-field approximation in laser-assisted dynamics
Am. J. Phys. **73**, 57 (2005); 10.1119/1.1796791

Strong-field non-sequential ionization: The vector momentum distribution of multiply charged Ne ions
AIP Conf. Proc. **525**, 285 (2000); 10.1063/1.1291947

Reuse of AIP Publishing content is subject to the terms: https://publishing.aip.org/authors/rights-and-permissions. Downloaded to IP: 115.156.232.60 On: Tue, 26 Apr 2016 02:38:07

The contribution of the delayed ionization in strong-field nonsequential double ionization

Yinbo Chen,[1] Yueming Zhou,[1,a)] Yang Li,[1] Min Li,[1] Pengfei Lan,[1] and Peixiang Lu[1,2,b)]
[1]*School of Physics, Huazhong University of Science and Technology, Wuhan 430074, People's Republic of China*
[2]*Laboratory of Optical Information Technology, Wuhan Institute of Technology, Wuhan 430205, People's Republic of China*

(Received 7 November 2015; accepted 24 December 2015; published online 11 January 2016)

With the classical ensemble model, we have investigated the pulse-duration dependence of nonsequential double ionization (NSDI) over a wide range of laser intensity. The correlated electron momentum distributions are distinctly different for the few-cycle and multiple cycle pulses, which agree well with the previous experiments. Based on this agreement, we analyzed the underlying process for the pulse-duration dependence of the electron correlation by tracing the classical trajectories. Counterintuitively, our analysis shows that the recollision-induced excited states of NSDI could resist ionization in the strong laser field for a time much longer than one optical cycle even at very high intensities. For the multiple-cycle pulses, NSDI events with such a long time delay have significant contribution to the total NSDI yields, which is responsible for the pulse-duration dependence of the observed correlated patterns in the electron momentum distributions. © *2016 AIP Publishing LLC.* [http://dx.doi.org/10.1063/1.4939642]

I. INTRODUCTION

Nonsequential double ionization (NSDI) is one of the most fundamental processes among various intense laser-induced phenomena.[1–6] It has drawn much attention since the first observation of the enhanced double ionization (DI) yield of rare gases.[7] The measurement of the electron or ion momenta[8–11] provided convincing evidences that the responsible mechanism of NSDI is the well-known recollision process.[12,13] In this process, the first electron ionized through tunneling is driven back to the parent ion when the electric field reverses its direction and kicks out the second electron through an inelastic recollision. Because of the recollision, the two ionized electrons exhibit a highly correlated behavior. Experimental and theoretical studies have shown that the details of the electron correlations sensitively depend on the laser intensity. For instance, at high laser intensities, the two electrons are most likely to emit into the same hemisphere, exhibiting a strong correlated behavior.[14–16] While at low laser intensities, the two electrons are more likely to emit into the opposite hemispheres and display an obvious anticorrelated behavior.[17] This intensity-dependent electron correlations reveal the different microscopic electron dynamics. With the development of laser techniques, intense few-cycle laser pulses with stable carrier envelope phase (CEP) are available.[18] In these few-cycle pulses, NSDI is confined to a single cycle of the pulses and thus the subcycle electron dynamics can be explored. Recently, numerous experimental studies have been performed on NSDI driven by few-cycle pulses.[19–23] It was shown that the correlated electron momentum distributions of NSDI by few-cycle pulses are distinctly different from those by the multiple-cycle pulses.[24] For example, at high laser intensity, the correlated electron momentum spectrum by the few-cycle pulses exhibits an impressive cross-shaped structure,[22] qualitatively differing from those by the multiple-cycle pulses.[11] At low laser intensity, a novel parallel-line structure was observed,[21] which has never been observed in the experiments using multiple-cycle pulses.

The laser intensity dependence of the electron correlations could be easily understood as the recollision induced direct ionization or excitation with subsequent ionization. Generally, at high laser intensities, the second electron is ionized directly by the recollision because of the high recollision energy.[25,26] At low laser intensities, the recollision energy is not high enough to kick out the second electron directly and thus NSDI can only occur through recollision-induced excited states.[27–31] The time delay between the ionization of the two electrons from the excited states determined the final electron correlations.[32,33] It is believed that usually these excited states were ionized in the strong laser field within one optical cycle.[22,27] Thus, it could be expected that the correlated electron dynamics of NSDI in few-cycle and multiple-cycle pulses should be similar. However, previous experiments, as mentioned above, show distinct difference of electron correlations between the few-cycle and multiple-cycle pulses. The underlying physics for this pulse-duration dependence of electron correlations is not intuitive.

In this paper, we performed a systematic study of NSDI of Ar over a wide range of laser intensities with different pulse durations, using the well-established classical ensemble model.[34,35] The correlated electron momentum distributions from our classical calculations are very different for the few-cycle and multiple cycle pulses, which are in very good

a)Electronic mail: zhouymhust@hust.edu.cn
b)Electronic mail: lupeixiang@hust.edu.cn

 © 2016 AIP Publishing LLC

Reuse of AIP Publishing content is subject to the terms: https://publishing.aip.org/authors/rights-and-permissions. Downloaded to IP: 115.156.232.60 On: Tue, 26 Apr 2016 02:38:07

agreement with previous experiments. Taking advantage of the classical method, we traced the time evolution of the NSDI trajectories and found that the recollision-induced excited states could stay in the laser fields for a time much longer than one optical cycle, even at very high laser intensities. Thus, for the multiple-cycle pulses, NSDI events with a time delay (the delay between final double ionization and recollision) much longer than one optical cycle have a significant contribution to the total NSDI yields, which is responsible for the pulse-duration dependence of electron correlations in the measured electron momentum spectra.

II. THE CLASSICAL ENSEMBLE MODEL

Accurate description of NSDI requires numerically solving the time-dependent Schrödinger equation. However, the computational demand of this method is huge and at present, it is only possible for some limited conditions.[36–38] In the past decades, classical methods have been proposed to study strong-field DI.[39–47] It has been confirmed that the classical methods are reliable tool in exploring microscopic electron dynamics in strong-field DI. For example, with the classical methods, the roles of the final-state electron-electron repulsion[44] and electron-ion attraction[44,48] in the measured electron spectra of NSDI are successfully identified, and the asymmetric energy sharing[49] during recollision has also been revealed. The classical methods are also successful in predicting new phenomena of strong-field DI.[50,51] Another important advantage of classical methods is that they can provide an intuitive picture of the underlying processes. Thus, in this paper, we employ the well-established classical ensemble model[34,39,40] proposed by Eberly *et al.* to study the electron dynamics of NDSI.

In this classical model, the core is fixed, and the evolution of the two-electron system is determined by the Newton's equations of motion[39] (atomic units are used throughout until stated otherwise),

$$\frac{\mathrm{d}^2\mathbf{r}_i}{\mathrm{d}t^2} = -\nabla[V_{ne}(\mathbf{r}_i) + V_{ee}(\mathbf{r}_1,\mathbf{r}_2)] - \mathbf{E}(t), \qquad (1)$$

where $\mathbf{r}_1$ and $\mathbf{r}_2$ denote the positions of the two electrons, and $\mathbf{E}(t) = E_0 \sin(\pi t/\tau)^2 \cos[\omega(t-\tau/2)+\phi]\hat{\mathbf{z}}$ is the electric field of the linearly polarized 790 nm laser pulses. E_0, τ, ω, and ϕ are the amplitude of the electric field, the pulse duration, the laser frequency, and the carrier envelope phase, respectively. The ion-electron and electron-electron potentials are represented as $V_{ne}(\mathbf{r}_i) = -2/\sqrt{\mathbf{r}_i^2 + a^2}$ and $V_{ee}(\mathbf{r}_1,\mathbf{r}_2) = 1/\sqrt{(\mathbf{r}_1-\mathbf{r}_2)^2+b^2}$. In order to avoid autoionization and the singularity of Coulomb potential, the screening parameters a = 1.5 and b = 0.05 are selected.[34,52] The initial state was obtained as follows. First, the two electrons of the model atom were placed at the classically allowed region of positions with an energy of −1.59 a.u., i.e., the sum of the first and second ionization potentials of Ar. The available kinetic energy was randomly distributed between the two electrons and the directions of the momenta were randomly assigned. Then the systems were allowed to evolve in the absence of laser field for a sufficiently long time (400 a.u.) to obtain stable distributions in the phase space. These distributions were the initial states of Eq. (1). Note that in this classical model, the species of the atomic target is only represented by the initial state energy. Once the initial state was obtained, the laser field was turned on. At the end of the laser pulses, we recorded the energies of electrons and DI was identified if both electrons achieved positive energies. In our calculations, the laser intensities were 0.8×10^{14} W/cm^2, 1.3×10^{14} W/cm^2, 2.3×10^{14} W/cm^2, which covered the area from the low to high laser intensity regions for NSDI of Ar.[27] We chose two different laser pulse durations of τ = 4T and τ = 16T (T is the laser cycle) to systematically study the pulse-duration-dependent NSDI dynamics at different laser intensities.

III. RESULTS

Figure 1 shows the correlated electron momentum spectra along the laser polarization direction for NSDI of Ar by laser pulses at the three different intensities. The pulse durations are τ = 4T and τ = 16T for the upper and lower rows, respectively. Here, the spectra for the 4T pulses were obtained by averaging over different CEPs, corresponding to the CEP-unlocked experiments. It can be seen that the electron correlations

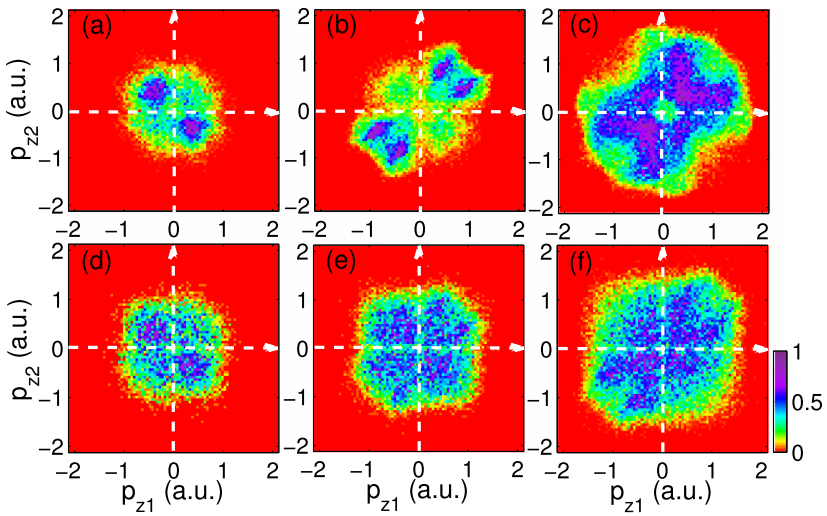

FIG. 1. Correlated electron momentum distributions along the laser polarization direction for NSDI of Ar by 790 nm laser pulses. The laser intensities are (a) and (d) 0.8×10^{14} W/cm^2, (b) and (e) 1.3×10^{14} W/cm^2, and (c) and (f) 2.3×10^{14} W/cm^2. The pulse durations are 4T and 16T for the upper and lower panels. The panels in the upper row are CEP averaged results. The ensemble sizes are several millions (depending on the laser intensity) so that as many as tens of thousands NSDI events are collected.

Reuse of AIP Publishing content is subject to the terms: https://publishing.aip.org/authors/rights-and-permissions. Downloaded to IP: 115.156.232.60 On: Tue, 26 Apr 2016 02:38:07

strongly depend on the laser intensity and the pulse duration. For the few-cycle pulses with the duration of 4T, the spectrum exhibits a strong anticorrelated pattern at low intensity of 0.8×10^{14} W/cm^2, as shown in Fig. 1(a). At relatively higher intensity of 1.3×10^{14} W/cm^2 [Fig. 1(b)], the distribution exhibits two lines nearly parallel to the main diagonal in the first and third quadrants. This parallel-line structure is in good agreement with the previous experimental result using pulse with similar laser parameters.[21] At high intensity of 2.3×10^{14} W/cm^2, as shown in Fig. 1(c), the spectrum exhibits a cross-shaped structure, which is also in good agreement with the experimental data.[22] For multiple-cycle pulses of 16T, as displayed in the lower row, the distributions are quite different from those of the few-cycle pulses. For example, at low intensity, the distribution also exhibits an anticorrelated behavior, but it is much weaker than that of the 4T pulse. At higher intensities [Figs. 1(e) and 1(f)], the parallel-line and cross-shaped structures observed in the case of few-cycle pulses [see Figs. 1(b) and 1(c)] are invisible at these long pulses. These results for the long pulses are in good agreement with the previous experimental data.[11,17]

For few-cycle pulses, because of the asymmetry of the electric field, the correlated electron momentum spectra for a fixed CEP should be asymmetric with respect to the diagonal $p_{z1} + p_{z2} = 0$.[19,21,22] We take the CEP $\phi = \pi$ to show this asymmetry, as presented in Fig. 2. The distribution is primarily clustered in the third quadrant for 1.3×10^{14} W/cm^2. For the intensity of 2.3×10^{14} W/cm^2, the distribution is also asymmetric but it is more likely to appear in the first quadrant [Fig. 2(c)]. This intensity dependence of the asymmetry has been analyzed in a previous paper.[53]

In order to explore the underlying dynamics of laser-intensity and pulse-duration dependence of the correlated behaviors of the electron pairs, we trace all classical trajectories of the NSDI events. In the following, we analyze the pulse-duration dependence of the correlated electron dynamics at the three laser intensities of 0.8×10^{14} W/cm^2, 1.3×10^{14} W/cm^2, and 2.3×10^{14} W/cm^2 one by one. We mention that these intensities are, respectively, corresponding to NSDI well below, close to and well above the threshold of direct ionization by recollision.

First, we focus on the low laser intensity of 0.8×10^{14} W/cm^2. Figure 3(a) shows the recollision time distribution for the 4T pulse, where the recollision time is defined as the instant of closest approach to the core after the ionization of the first electron.[34] Here, the CEP was set to be $\phi = \pi$. As shown in Fig. 3(a), the recollision occurs just after the electric field peak at 2.0T. Due to the low laser intensity, the recollision electron excites the bound electron at the expense of being recaptured by the core, forming a doubly excited state.[32,33] After that the two electrons are ionized by the following electric field one after the other. Figure 3(c) shows

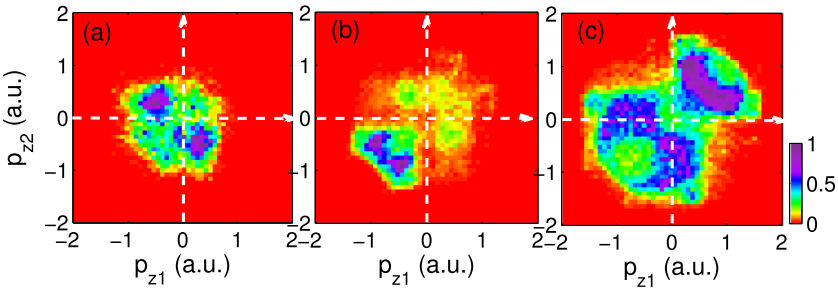

FIG. 2. The correlated electron momentum distributions for 4T pulses with CEP $\phi = \pi$. The laser intensities are (a) 0.8×10^{14} W/cm^2, (b) 1.3×10^{14} W/cm^2, and (c) 2.3×10^{14} W/cm^2.

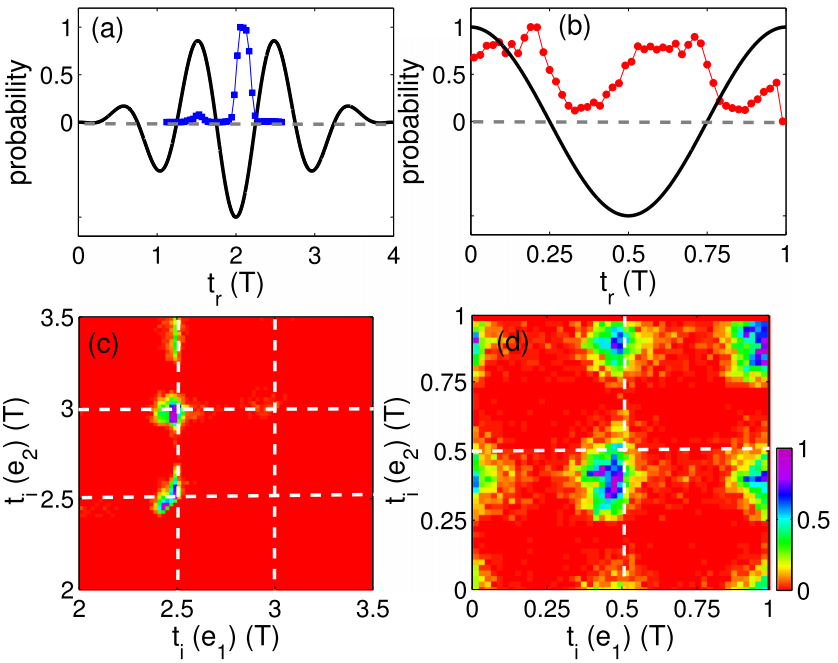

FIG. 3. (a) Recollision time distribution of the NSDI events for the 4T pulse (blue squares). (b) Relative proportion of NSDI trajectories versus laser phase at time of recollision for the 16T pulse (red circles). (c) Final ionization time of the first versus the second electrons for the 4T pulse. (d) Laser phase at the ionization of the first versus the second electrons for the 16T pulse. The first and the second electrons are classified based on the ionization order after recollision. The black solid lines in (a) and (b) denote the electric field and the dashed lines in (c) and (d) indicate the peaks of the electric field. The laser intensity is 0.8×10^{14} W/cm^2. The CEP of the 4T pulse is $\phi = \pi$.

Reuse of AIP Publishing content is subject to the terms: https://publishing.aip.org/authors/rights-and-permissions. Downloaded to IP: 115.156.232.60 On: Tue, 26 Apr 2016 02:38:07

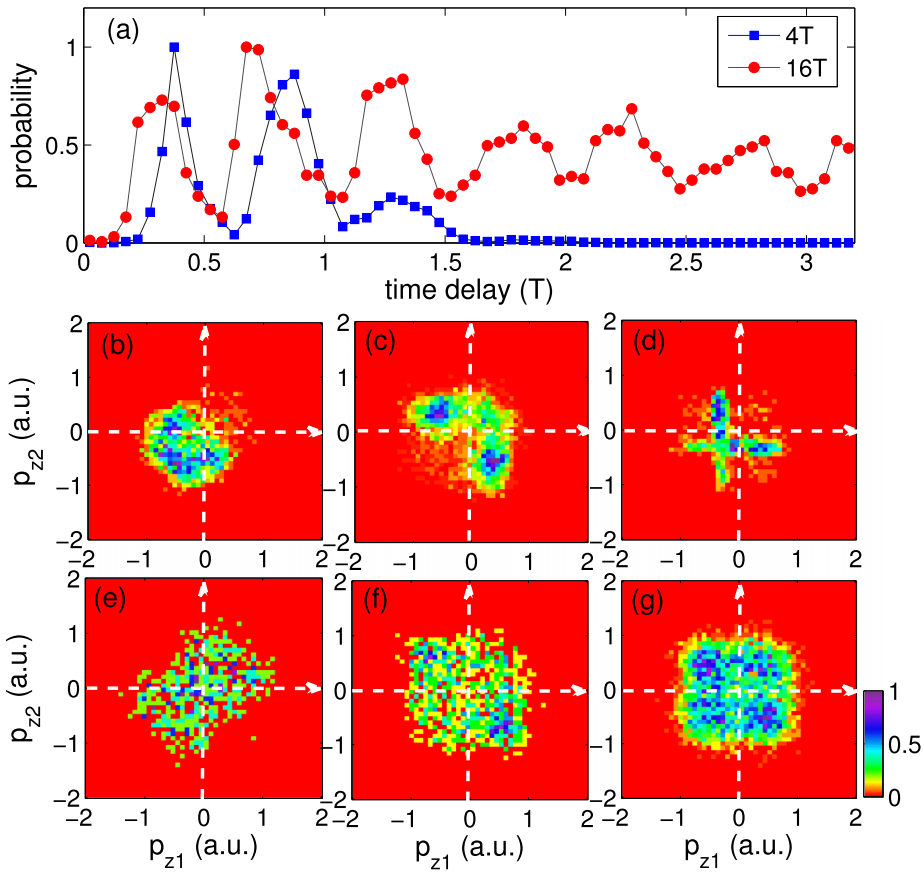

FIG. 4. (a) The distribution of time delay between DI and recollision. The blue squares and red circles represent the results for the 4T and 16T pulses, respectively. (b)-(d) Correlated electron momentum distributions of the 4T pulse for the NSDI with time delay of (b) 0-0.5T, (c) 0.6-1.0T, and (d) longer than 1.0T. (e)-(g) The same as (b)-(e) but for the 16T pulse. In each panel the distribution is normalized. The CEP of the 4T pulse is $\phi = \pi$. The laser intensity is 0.8×10^{14} W/cm^2.

the final ionization time of the two electrons after recollision, where the final ionization time is defined as the instant when the electron achieves positive energy after recollision. Here we labeled the electrons as the first and the second electrons based on the ionization order after the recollision. It is shown that for the first electron, ionization occurs just before the first electric field peak (at 2.5T) following recollision. For the second electron, ionization most likely occurs around the first or the second electric field peaks following recollision. For the long pulse, we considered the laser phase at time of recollision and ionization.[33] Figure 3(b) displays the laser phase at the times of recollision for the 16T pulse. It is shown that recollision occurs at the time between the maximum and zero crossing of the electric field. The laser phases of final ionizations of the first and the second electrons are shown in Fig. 3(d), indicating that both electrons are ionized just before or around the peaks of the following electric field.

It is known that the final correlated pattern of the electron pairs depends on the time delay between final ionizations of the two electrons and the recollision.[32,33] In Fig. 4(a), we present the time delay between DI (the instant when both electrons achieve positive energies) and recollision for the 4T (blue squares) and 16T (red circles) pulses. For these two pulses, the distributions exhibit similar behavior for the first three peaks. For example, the first, second, and third peaks locate near 0.3T, 0.75T, and 1.25T, respectively. For the long pulse, there are a significant part of events with a very large time delay, indicating that the second excited electron survived in the laser field for a long time. In the middle and bottom rows of Fig. 4, we plotted the correlated electron spectra according to the time delay for the 4T and 16T pulses, respectively. Figs. 4(b) and 4(e) correspond to the events with a time delay of 0-0.5T [the first peak in Fig. 4(a)], and Figs. 4(c) and 4(f) show these with a time delay of 0.6T-1.0T [the second peak in Fig. 4(a)]. It is shown that for the events with a similar time delays, the correlated electron momentum spectra are similar for the 4T and 16T pulses. For example, in Figs. 4(b) and 4(e), the distributions exhibit a correlated behavior and in Figs. 4(c) and 4(f), they show an anticorrelated behavior. Note that for the 4T pulse, the CEP was set to be $\phi = \pi$ and thus the spectra are asymmetric with respect to the diagonal $p_{z1} + p_{z2} = 0$. So the distribution only appears in the area below this diagonal. In Figs. 4(d) and 4(g), we display the correlated electron momentum spectra for the events with a time delay longer than 1.0T. It is clearly shown that for the 4T pulse, the distribution is dominantly clustered in the second and fourth quadrants. However, for the 16T pulse, because of the multiple peaks in the time delay distribution of Fig. 4(a), the correlated electron spectrum exhibits a nearly uniform distribution and this part of events has the significant contribution to the total NSDI yields. Thus, we can conclude that the difference in the correlated electron momentum spectra for the few-cycle and multiple-cycle pulses is due to the fact that in multiple-cycle pulses, there are significant contribution of NSDI events with time delay much longer than one optical cycle.

Now, we turn to the higher laser intensity of 1.3×10^{14} W/cm^2. For this intensity, it has been shown that the main part of NSDIs also occurs through the recollision-induced doubly excited states.[21] In Figs. 5(a) and 5(b), we show the recollision time distributions for the 4T and 16T pulses,

Reuse of AIP Publishing content is subject to the terms: https://publishing.aip.org/authors/rights-and-permissions. Downloaded to IP: 115.156.232.60 On: Tue, 26 Apr 2016 02:38:07

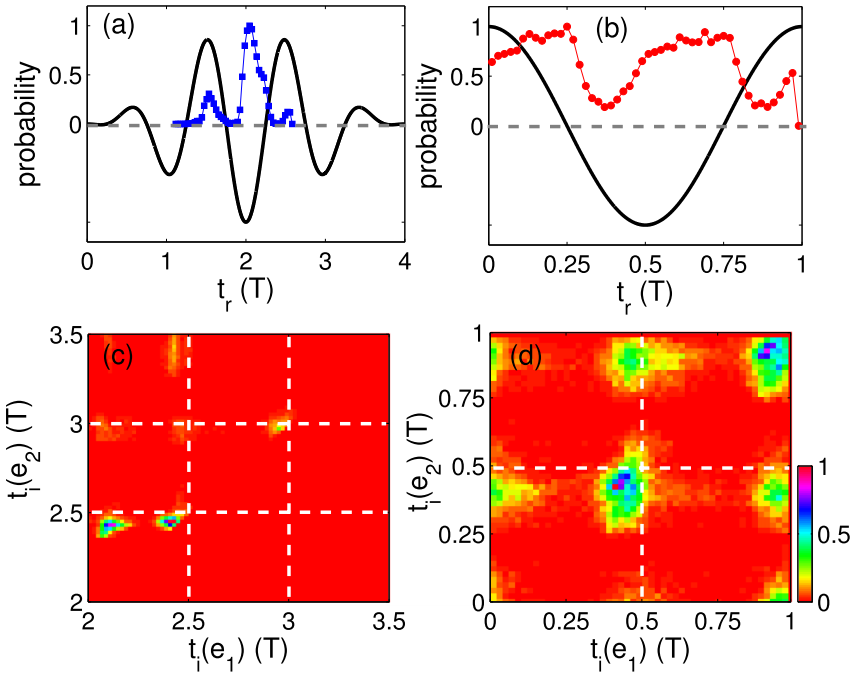

FIG. 5. The same as Fig. 3 but for the intensity of 1.3×10^{14} W/cm^2.

respectively. These distributions are very similar to those in Figs. 3(a) and 3(b). Figure 5(c) displays the final ionization time of the two electrons after recollision for the 4T pulse. It is shown that for the first electron, ionization occurs just after the recollision (2.0T) or before the first electric field peak (2.5T) following recollision. For the second electron, final ionization occurs just before the first electric field peak (2.5T) following recollision. For this type of trajectories, the two electrons emit in the same direction along the laser polarization. Due to the time delay between the final ionizations of the two electrons[21] and the electron repulsion between them,[54] the final correlated electron momentum spectrum exhibits a double-line structure in the first and third quadrants [Fig. 1(b)]. For the long pulse of 16T, recollision also mainly occurs between the peaks and zero crossings of the electric field, as shown in Fig. 5(b), and final ionizations of both electrons happen just before the peaks of the electric field [Fig. 5(d)]. These behaviors are similar to those at lower laser intensity in Fig. 3.

In Fig. 6(a), we display the time delay between DI and recollision. Again, these time delay distributions for the 4T and 16T pulses are very similar for the first peak. For the 16T pulse, there are considerable NSDI events with a time

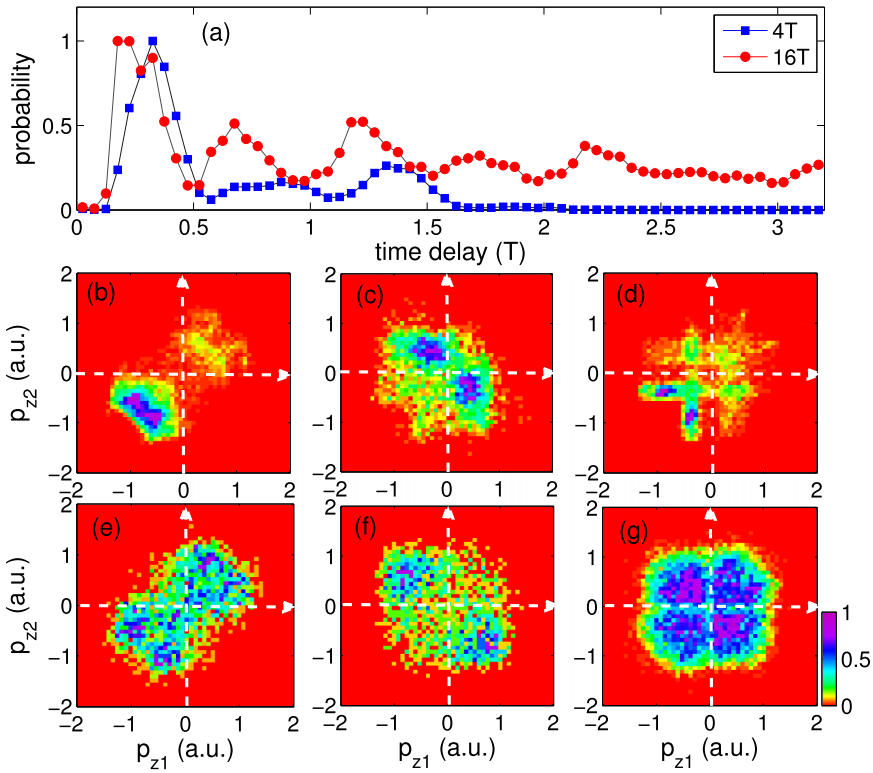

FIG. 6. The same as Fig. 4 but for the intensity of 1.3×10^{14} W/cm^2.

Reuse of AIP Publishing content is subject to the terms: https://publishing.aip.org/authors/rights-and-permissions. Downloaded to IP: 115.156.232.60 On: Tue, 26 Apr 2016 02:38:07

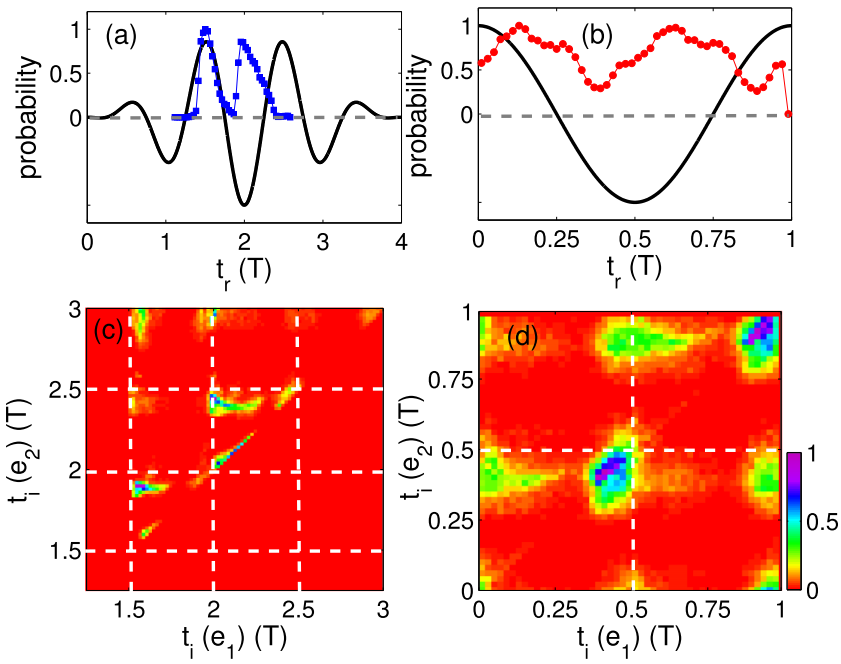

FIG. 7. The same as Fig. 3 but for the intensity of 2.3×10^{14} W/cm^2.

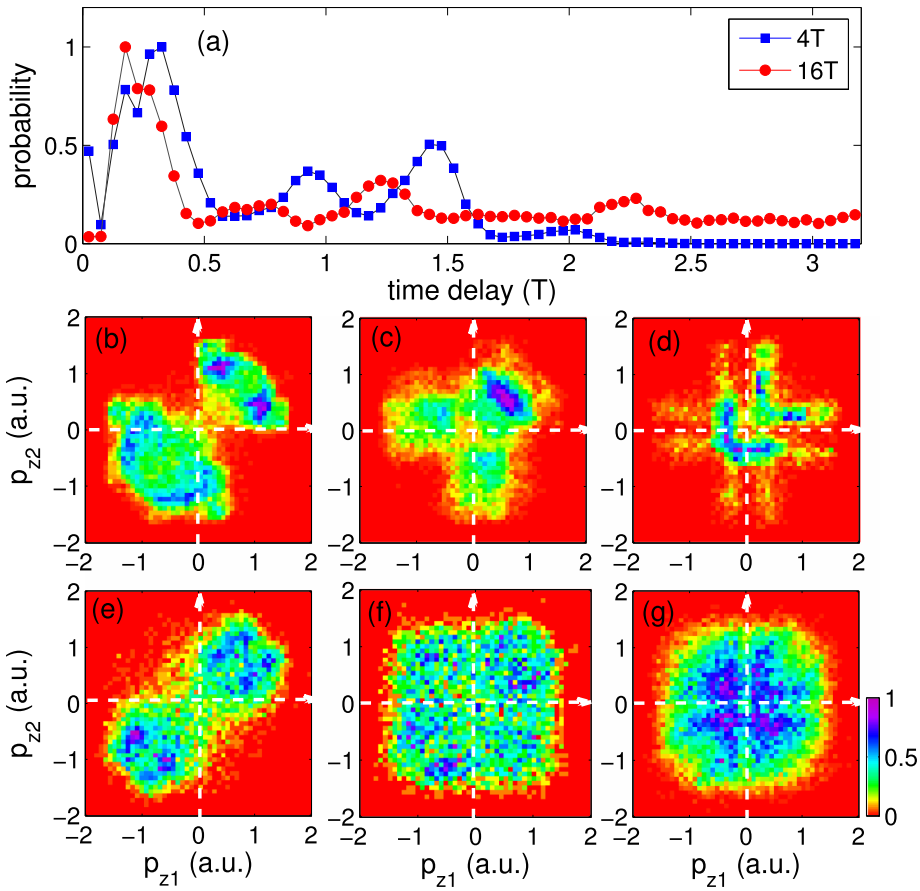

FIG. 8. (a) The same as Fig. 4(a) but for the intensity of 2.3×10^{14} W/cm^2. (b)-(e) Correlated electron momentum distributions of the 4T pulse for the NSDI with time delay of (b) 0-0.5T, (c) 0.5-1.5T, and (d) longer than 1.5T. (e)-(g) The same as (b)-(e) but for the 16T pulse. In each panel, the distribution is normalized so that the maximum value is unit.

delay much longer than one optical cycle. In the middle and bottom rows of Fig. 6, we separately plotted the correlated electron momentum distributions of the NSDI events with different time delays for the 4T and 16T pulses, respectively. Figures 6(b) and 6(e) represent these with a time delay less than 0.5T [the first peak in Fig. 6(a)] for the 4T and 16T pulses, respectively. It is shown that the distributions are very similar for these two pulses, i.e., both distributions exhibit a clear repulsion behavior along the main diagonal $p_{z1} = p_{z2}$. Figures 6(c) and 6(d) display the distributions for the NSDI events with a time delay of 0.5T-1.0T. For both pulses, the distributions exhibit an anticorrelated behavior. Figures 6(d) and 6(g) show the distributions for the NSDI events with the time delay longer than 1.0T. For the 16T pulse [Fig. 6(g)], the double-line structure is invisible. Note that the proportion of this part in the total NSDI yield is negligible for the 4T

Reuse of AIP Publishing content is subject to the terms: https://publishing.aip.org/authors/rights-and-permissions. Downloaded to IP: 115.156.232.60 On: Tue, 26 Apr 2016 02:38:07

pulse while it is significant for the 16T pulse. Because of the contribution of this type of NSDI events in the 16T pulse, the double-line structure shown in Fig. 6(e) is seriously obscured. Therefore, the double-line structure observed in the few-cycle pulses is invisible in the multiple-cycle pulses.

Figures 7 and 8 show the results at the high laser intensity of 2.3×10^{14} W/cm^2. At this laser intensity, there are two bursts of recollision in the 4T pulse [Fig. 7(a)] and the distribution for the 16T pulse [Fig. 7(b)] is wider than that at lower laser intensities. It is shown in Fig. 7(c) that there are many events along the diagonal, meaning that the two electrons ionizes simultaneously after recollision. There are also a significant part of events where the second electron ionize just before the electric field peaks at 2.0T and 2.5T, indicating that NSDI occurs through the recollision-excitation ionization process even at this high laser intensity. This is consistent with previous study.[22]

Figure 8 depicts the correlated momentum distributions of the NSDI events with different time delays between DI and recollision. Figure 8(a) gives the time delay distributions for the 4T and 16T pulses. It is more directly shown here that there is a significant time delay between DI and recollision for both pulse durations, confirming again the recollision-excitation-ionization process in the high laser intensity regime.[22] Figures 8(b) and 8(e) show the spectra for the NSDI events with time delay less than 0.5T [the first peak in Fig. 8(a)] for the 4T and 16T pulses, respectively. Figures 8(c) and 8(f) present the NSDI events with time delay of 0.5T-1.5T. Again, the spectra of the 4T and 16T pulses are similar for the NSDI events with same time delay. For the 4T pulse, the contribution of NSDI events with time delay longer than 1.5T is negligible while for the 16T pulse, the events with this long time delay take a very large proportion of the total NSDI yields. The correlated electron spectra for the events with time delay longer than 1.5T are shown in Figs. 8(d) and 8(g). Obviously, this part is the main reason for the difference in the correlated electron momentum distributions for the 4T and 16T pulses, as shown in Figs. 1(c) and 1(f).

IV. CONCLUSION

In summary, we have systematically investigated the pulse-duration dependence of NSDI over a wide range of laser intensity. The results from our classical ensemble model are in good agreement with previous experimental data. Back tracing of the NSDI trajectories shows that the recollision-excited electrons can resist ionization for a time much longer than one optical cycle, even at the laser intensities well above the recollision-ionization threshold. Consequently, for the multiple-cycle pulses, the contribution of NSDI events with a very long time delay after recollision is significant. This is responsible for the difference in the observed correlated electron momentum spectra of the few-cycle and multiple-cycle pulses.

ACKNOWLEDGMENTS

This work was supported by the National Natural Science Foundation of China under Grant Nos. 61405064 and 11234004. Numerical simulations presented in this paper were carried out using the High Performance Computing Center experimental testbed in SCTS/CGCL (see http://grid.hust.edu.cn/hpcc).

[1]W. Becker, F. Grasbon, R. Kopold, D. Milošević, G. Paulus, and H. Walther, Adv. At., Mol., Opt. Phys. **48**, 35-98 (2002).
[2]F. Krausz and M. Ivanov, Rev. Mod. Phys. **81**, 163-234 (2009).
[3]L. He, P. Lan, Q. Zhang, C. Zhai, F. Wang, W. Shi, and P. Lu, Phys. Rev. A **92**, 043403 (2015).
[4]Q. Liao, Y. Zhou, C. Huang, and P. Lu, New J. Phys. **14**, 013001 (2012).
[5]M. Li, P. Zhang, S. Luo, Y. Zhou, Q. Zhang, P. Lan, and P. Lu, Phys. Rev. A **92**, 063404 (2015).
[6]Y. Li, P. Lan, H. Xie, M. He, X. Zhu, Q. Zhang, and P. Lu, Opt. Express **23**, 28801-28807 (2015).
[7]A. I'Huillier, L. A. Lompre, G. Mainfray, and C. Manus, Phys. Rev. A **27**, 2503-2512 (1983).
[8]Th. Weber, M. Weckenbrock, A. Staudte, L. Spielberger, O. Jagutzki, V. Mergel, F. Afaneh, G. Urbasch, M. Vollmer, H. Giessen, and R. Dörner, Phys. Rev. Lett. **84**, 443-446 (2000).
[9]R. Moshammer, B. Feuerstein, W. Schmitt, A. Dorn, C. D. Schröter, J. Ullrich, H. Rottke, C. Trump, M. Wittmann, G. Korn, K. Hoffmann, and W. Sandner, Phys. Rev. Lett. **84**, 447-450 (2000).
[10]A. Rudenko, K. Zrost, B. Feuerstein, V. L. B. de Jesus, C. D. Schröter, R. Moshammer, and J. Ullrich, Phys. Rev. Lett. **93**, 253001 (2004).
[11]Th. Weber, H. Giessen, M. Weckenbrock, G. Urbasch, A. Staudte, L. Spielberger, O. Jagutzki, V. Mergel, M. Vollmer, and R. Dörner, Nature **405**, 658-661 (2000).
[12]K. J. Schafer, B. Yang, L. I. DiMauro, and K. C. Kulanderc, Phys. Rev. Lett. **70**, 1599-1602 (1993).
[13]P. B. Corkum, Phys. Rev. Lett. **71**, 1994-1997 (1993).
[14]M. Weckenbrock, D. Zeidler, A. Staudte, Th. Weber, M. Schöffler, M. Meckel, S. Kammer, M. Smolarski, O. Jagutzki, V. R. Bhardwaj, D. M. Rayner, D. M. Villeneuve, P. B. Corkum, and R. Dörner, Phys. Rev. Lett. **92**, 213002 (2004).
[15]A. Staudte, C. Ruiz, M. Schöffler, S. Schössler, D. Zeidler, Th. Weber, M. Meckel, D. M. Villeneuve, P. B. Corkum, A. Becker, and R. Dörner, Phys. Rev. Lett. **99**, 263002 (2007).
[16]A. Rudenko, V. L. B. de Jesus, Th. Ergler, K. Zrost, B. Feuerstein, C. D. Schröter, R. Moshammer, and J. Ullrich, Phys. Rev. Lett. **99**, 263003 (2007).
[17]Y. Liu, S. Tschuch, A. Rudenko, M. Dürr, M. Siegel, U. Morgner, R. Moshammer, and J. Ullrich, Phys. Rev. Lett. **101**, 053001 (2008).
[18]G. G. Paulus, F. Grasbon, H. Walther, P. Villoresi, M. Nisoli, S. Stagira, E. Priori, and S. De Silvestri, "Absolute-phase phenomena in photoionization with few-cycle laser pulses," Nature **414**, 182-184 (2001).
[19]X. Liu, H. Rottke, E. Eremina, W. Sandner, E. Goulielmakis, K. O. Keeffe, M. Lezius, F. Krausz, F. Lindner, M. G. Schätzel, G. G. Paulus, and H. Walther, Phys. Rev. Lett. **93**, 263001 (2004).
[20]N. Johnson, O. Herrwerth, A. Wirth, S. De, I. Ben-Itzhak, M. Lezius, B. Bergues, M. F. Kling, A. Senftleben, C. D. Schröter, R. Moshammer, J. Ullrich, K. J. Betsch, R. R. Jones, A. M. Sayler, T. Rathje, K. Rhle, W. Müller, and G. G. Paulus, Phys. Rev. A **83**, 013412 (2011).
[21]N. Camus, B. Fischer, M. Kremer, V. Sharma, A. Rudenko, B. Bergues, M. Kübel, N. G. Johnson, M. F. Kling, T. Pfeifer, J. Ullrich, and R. Moshammer, Phys. Rev. Lett. **108**, 073003 (2012).
[22]B. Bergues, M. Kbel, N. G. Johnson, B. Fischer, N. Camus, K. J. Betsch, O. Herrwerth, A. Senftleben, A. Max Sayler, T. Rathje, T. Pfeifer, I. Ben-Itzhak, R. R. Jones, G. G. Paulus, F. Krausz, R. Moshammer, J. Ullrich, and M. F. Kling, Nat. Commun. **3**, 813 (2012).
[23]M. Kübel, N. Kling, K. J. Betsch, N. Camus, A. Kaldun, U. Kleineberg, I. Ben-Itzhak, R. R. Jones, G. G. Paulus, T. Pfeifer, J. Ullrich, R. Moshammer, M. F. Kling, and B. Bergues, Phys. Rev. A **88**, 023418 (2013).
[24]M. Kübel, K. J. Betsch, N. G. Kling, A. S. Alnaser, J. Schmidt, U. Kleineberg, Y. Deng, I. Ben-Itzhak, G. G. Paulus, T. Pfeifer, J. Ullrich, R. Moshammer, M. F. Kling, and B. Bergues, New J. Phys. **16**, 033008 (2014).
[25]R. Kopold, W. Becker, H. Rottke, and W. Sandner, Phys. Rev. Lett. **85**, 3781 (2000).
[26]Y. Zhou, Q. Liao, and P. Lu, Opt. Express **18**, 16025-16034 (2010).
[27]B. Feuerstein, R. Moshammer, D. Fischer, A. Dorn, C. D. Schröter, J. Deipenwisch, J. R. Crespo Lopez-Urrutia, C. Höhr, P. Neumayer, J. Ullrich, H. Rottke, C. Trump, M. Wittmann, G. Korn, and W. Sandner, Phys. Rev. Lett. **87**, 043003 (2001).
[28]A. Emmanouilidou and A. Staudte, Phys. Rev. A **80**, 053415 (2009).

Reuse of AIP Publishing content is subject to the terms: https://publishing.aip.org/authors/rights-and-permissions. Downloaded to IP: 115.156.232.60 On: Tue, 26 Apr 2016 02:38:07

[29]C. Faria, T. Shaaran, and M. T. Nygren, Phys. Rev. A **86**, 053405 (2012).
[30]X. Hao, J. Chen, W. Li, B. Wang, X. Wang, and W. Becker, Phys. Rev. Lett. **112**, 073002 (2014).
[31]A. S. Maxwell and C. Figueira de Morisson Faria, Phys. Rev. A **92**, 023421 (2015).
[32]S. L. Haan, Z. S. Smith, K. N. Shomsky, and P. W. Plantinga, J. Phys. B **41**, 211002 (2008).
[33]Y. Zhou, C. Huang, and P. Lu, Phys. Rev. A **84**, 023405 (2011).
[34]S. L. Haan, L. Breen, A. Karim, and J. H. Eberly, Phys. Rev. Lett. **97**, 103008 (2006).
[35]Y. Zhou, Q. Liao, and P. Lu, Phys. Rev. A **80**, 023412 (2009).
[36]J. S. Parker, B. J. S. Doherty, K. T. Taylor, K. D. Schultz, C. I. Blaga, and L. F. DiMauro, Phys. Rev. Lett. **96**, 133001 (2006).
[37]S. Hu, Phys. Rev. Lett. **111**, 123003 (2013).
[38]A. Liu and U. Thumm, Phys. Rev. A **89**, 063423 (2014).
[39]R. Panfili, J. Eberly, and S. Haan, Opt. Express **8**, 431-435 (2001).
[40]P. J. Ho, R. Panfili, S. L. Haan, and J. H. Eberly, Phys. Rev. Lett. **94**, 093002 (2005).
[41]Y. Zhou, C. Huang, Q. Liao, W. Hong, and P. Lu, Opt. Lett. **36**, 2758-2760 (2011).
[42]F. Mauger, C. Chandre, and T. Uzer, Phys. Rev. Lett. **105**, 083002 (2010).
[43]A. Emmanouilidou, J. S. Parker, L. R. Moore, and K. T. Taylor, New J. Phys. **13**, 043001 (2011).
[44]D. Ye, X. Liu, and J. Liu, Phys. Rev. Lett. **101**, 233003 (2008).
[45]Y. Zhou, C. Huang, Q. Liao, and P. Lu, Phys. Rev. Lett. **109**, 053004 (2012).
[46]Y. Zhou, C. Huang, Q. Liao, and P. Lu, Phys. Rev. A **86**, 043427 (2012).
[47]T. Wang, X. Ge, J. Guo, and X. Liu, Phys. Rev. A **90**, 033420 (2014).
[48]S. L. Haan, J. Dyke, and Z. Smith, Phys. Rev. Lett. **101**, 113001 (2008).
[49]Y. Zhou, Q. Liao, and P. Lu, Phys. Rev. A **82**, 053402 (2010).
[50]A. Tong, Y. Zhou, and P. Lu, Opt. Express **23**, 15774-15783 (2015).
[51]Y. Zhou, C. Huang, A. Tong, Q. Liao, and P. Lu, Opt. Express **19**, 2301-2308 (2011).
[52]C. Huang, Y. Zhou, Q. Zhang, and P. Lu, Opt. Express **21**, 11382-11390 (2013).
[53]H. Li, J. Chen, H. Jiang, J. Liu, P. Fu, Q. Gong, Z. Yan, and B. Wang, Opt. Express **16**, 20562-20570 (2008).
[54]C. Huang, W. Guo, Y. Zhou, and Z. Wu, "Role of Coulomb repulsion in correlated-electron emission from a doubly excited state in nonsequential double ionization of molecules" (to be published).

Reuse of AIP Publishing content is subject to the terms: https://publishing.aip.org/authors/rights-and-permissions. Downloaded to IP: 115.156.232.60 On: Tue, 26 Apr 2016 02:38:07